Alisol A is potentially therapeutic in human breast cancer cells

YANYAN SHI[1*], MOPEI WANG[2*], PAN WANG[3*], TING ZHANG[4], JINGYI YU[5], LUNYONG SHI[5], MO LI[3], HAO WANG[6], QINGYING ZHANG[5] and HONGMEI ZHAO[7]

[1]Peking University Third Hospital, Research Center of Clinical Epidemiology; [2]Peking University Third Hospital, Department of Tumor Chemotherapy and Radiation Sickness; [3]Peking University Third Hospital, Department of Obstetrics and Gynecology; [4]Peking University Health Science Center, Department of Microbiology; [5]Peking University Health Science Center, School of Pharmaceutical Sciences, Department of Natural Medicines, Beijing 100191; [6]Sun Yat-Sen Memorial Hospital of Sun Yat-Sen University, Department of Obstetrics and Gynecology, Guangzhou, Guangdong 510120; [7]Peking University Third Hospital, Department of General Surgery, Beijing 100191, P.R. China

Received December 23, 2019; Accepted May 19, 2020

DOI: 10.3892/or.2020.7654

Abstract. Recent developments in breast cancer therapy have significantly improved patient survival rate; however, recurrence remains a major problem. Systemic treatment of breast cancer with available therapies is not curative. Natural products can be potentially used for treating cancer. Recently, a wide range of pharmacological activities has been reported for Alismatis Rhizoma, a popular traditional Chinese medicine. However, the mechanisms via which its compounds act on breast cancer remain unclear. The present study aimed to investigate the potential of natural therapeutic agents from Alismatis Rhizoma for treating breast cancer. Human breast cancer MDA-MB-231 cells were treated with four main protostane triterpenes from Alismatis Rhizoma, including alisol A, alisol A 24-acetate, alisol B and alisol B 23-acetate. Among these, alisol A significantly inhibited cell viability. Alisol A induced cell apoptosis, G_1 phase cell cycle arrest, autophagy, and intracellular reactive oxygen species (ROS) generation in MDA-MB-231 cells. The number of APE1-/γH2AX-/LC3-II positive cells was also significantly higher compared with that of negative control cells. All these results were dose-dependent. Cleaved caspase-3, cleaved caspase 9, Bcl-2, and p-p38 expression indicated cell apoptosis after alisol A treatment. The changes in cyclin A and cyclin D1 expression was associated with cell cycle arrest upon alisol A treatment. Furthermore, LC3-II expression upon alisol A treatment was indicative of autophagy. Alisol A treatment can induce autophagy-dependent apoptosis in human breast cancer cells via induction of ROS and DNA damage. Thus, Alisol A might serve as a new therapeutic agent against breast cancer.

Correspondence to: Dr Hongmei Zhao, Peking University Third Hospital, Department of General Surgery, 49 Garden North Road, Haidian, Beijing 100191, P.R. China
E-mail: zhao_hm118@163.com

Professor Qingying Zhang, Peking University Health Science Center, School of Pharmaceutical Sciences, Department of Natural Medicines, 38 Xueyuan Road, Haidian, Beijing 100191, P.R. China
E-mail: qyzhang@hsc.pku.edu.cn

*Contributed equally

Abbreviations: TNBC, triple-negative breast cancer; TUNEL, terminal deoxynucleotidyl transferase-mediated dUTP nick-end labeling; PI, propidium iodide; APE1, apurinic/apyrimidinic endonuclease 1; γH2AX, phosphorylated H2AX; ROS, reactive oxygen species; DNA, deoxyribonucleic acid; HPLC, high performance liquid chromatography; UV, ultraviolet; FITC, fluorescein isothiocyanate isomer I; DMSO, dimethyl sulfoxide; 7AAD, 7-amino-actinomycin D; DCF-DA, 2',7'-dichlorodihydrofluorescein diacetate; PBS, phosphate buffer saline; DAPI, 4'6-diamidino-2-phenylindole; p-p38, phosphorylated p38

Key words: Alismatis Rhizoma, alisol A, breast cancer, apoptosis, autophagy, DNA damage

Introduction

Breast cancer is the most commonly diagnosed cancer and the leading cause of cancer-associated death among women in most countries (1). In both developed and developing countries, the incidence rates of breast cancer far exceed those for other cancer types in women. Based on the 2008 and 2010 data, one in eight women in the USA has the risk of being diagnosed with breast cancer in her lifetime, compared with the lifetime risk of one in eleven in the 1970s (2). In women, the incidence of breast cancer is considerably higher in comparison to other cancer types. The incidence rate of breast cancer has increased over the last few decades in most countries (3). For example, the incidence rates have increased rapidly in Asia, Africa, and South America, where they had been relatively low in the past. The primary risk factors for breast cancer cannot be modified easily, as these factors are associated with prolonged, endogenous hormonal exposures (1). Hence, advanced therapeutic studies on breast cancer are urgently required.

Recent developments in breast cancer chemotherapy have significantly improved patient survival rates; however, the recurrence of breast cancer remains a major problem. Systemic treatment of breast cancer with available therapies is not curative (4). Triple-negative breast cancer (TNBC) is highly heterogeneous, comprising approximately 10-20% of all breast cancer cases, and frequently occurs in women younger than 50 years of age (5). The prognosis of TNBC is the poorest among all types of breast cancer, due to limited treatment options. Recently, novel therapies like nanotherapeutics have been developed to improve the efficacy and decrease the toxicity of antitumor drugs (6). However, the heterogeneity and complexities of tumors hinder the widespread clinical application of nanomedicine. None of the nanotherapeutics used clinically is tumor specific, and targeted therapies for TNBC are still at their early stage (7).

In order to address the aforementioned challenges, new drugs for breast cancer therapy are urgently required. Natural products with a wide range of physiological activities can be used for treating specific diseases. Natural products have contributed significantly to the discovery and development of new drugs, especially those for cancer therapy (8,9). Alismatis Rhizoma, a popular traditional Chinese medicine derived from the dried rhizome of *Alisma orientale* (Sam.) Juz, is recorded in Shen Nong's Herbal Classic and has been used for removing dampness and promoting urination for thousands of years (10). Recently, a wide range of pharmacological activities has been reported for Alismatis Rhizoma, including removal of dampness and elimination of edema, promotion of water metabolism, and anti-hyperlipidemia, anti-complementary, antioxidant, and anti-cancer properties (11). Phytochemical investigations have revealed that protostane triterpenes are the principal constituents of Alismatis Rhizoma, which are considered to be responsible for its various efficacies (12). However, the mechanisms via which its compounds act on breast cancer remain unclear.

In the present study, the effects of four main protostane triterpenes of Alismatis Rhizoma, including alisol A, alisol A 24-acetate, alisol B, and alisol B 23-acetate, were investigated in breast cancer cells. Alisol A showed significant anticancer effects in MDA-MB-231 breast cancer cells, which is a TNBC breast cancer cell line. The mechanisms of action of alisol A on this cell line were also investigated. The results will provide a comprehensive understanding regarding the anticancer effects of alisol A in human breast cancer cells.

Materials and methods

Ethics. The use of human specimens in the present study was approved by the Peking University Third Hospital Medical Science Research Ethic Committee (approval no. IRB00006761-M2019343). Informed consent was signed by all the patients.

Chemicals. Four protostane triterpenes, namely, alisol A, alisol A 24-acetate, alisol B, and alisol B 23-acetate, were purified from Alismatis Rhizoma by repeated chromatography on silica gel, reversed-phase C18, Sephadex LH-20, and semi-preparative RP-C18 high performance liquid chromatography (HPLC), and their structures were characterized based on comprehensive nuclear magnetic resonance, mass spectroscopy, and ultraviolet (UV) spectral analysis. The purity of the four compounds was greater than 98%, as assessed after normalization of the HPLC-UV peaks observed at 210 nm (Fig. S1).

Cell culture and treatment. Human breast cancer MDA-MB-231 cells, from American Type Culture Collection, were cultured in Dulbecco's modified Eagle's medium (DMEM; Gibco; Thermo Fisher Scientific, Inc.) supplemented with 10% (v/v) fetal bovine serum (FBS) (HyClone; Cytvia), 100 U/ml penicillin and streptomycin. MDA-MB-231 cells were cultured at 37˚C in a humidified incubator in the presence of 5% (v/v) CO_2. After the cells reached 80% confluence, cells were detached using trypsin (HyClone; Cytvia), counted, and plated at the necessary density for treatment. Primary human TNBC breast cancer cells were isolated from tumor specimens, lesion was 1x1x0.2 cm from a 56-year-old patient diagnosed with breast invasive ductal carcinoma in July 2019, and cultured in DMEM/F12 supplemented with 5% (v/v) FBS, 0.4 μg/ml hydrocortisone (Sigma-Aldrich; Merck KGaA), 1X Insulin-Transferrin-Selenium (Sigma-Aldrich; Merck KGaA), 10 ng/ml epidermal growth factor (EGF) (Invitrogen; Thermo Fisher Scientific, Inc.), 25 μg/ml adenine (Sigma-Aldrich; Merck KGaA), 10 ng/ml cholera toxin (Sigma-Aldrich; Merck KGaA), and 10 μmol/l Y-27632 (MedChemExpress). Alisol A, alisol A 24-acetate, alisol B, or alisol B 23-acetate were used to treat cells for 24 h.

Real-time cell viability assay. A real-time cell proliferation assay was conducted using the ACEA RT-CES microelectronic cell sensor system (ACEA Bioscience, Inc.) to measure the numbers of living cells. This system works by measuring electrical impedance of sensor electrodes integrated on the bottom of microtiter E-plates as previously described (13). Briefly, after treatment with 5, 10 or 20 μM compounds for 24 h, $5x10^3$ breast cancer cells per well, including MDA-MB-231 cells and primary human TNBC cells, were seeded in E-Plate 96 at 37˚C in a humidified incubator in the presence of 5% (v/v) CO_2 and allowed to attach for 12 h. A unitless parameter termed the cell index was derived and used to represent the cell numbers, based on the measured relative changes in electrical impedance that occurred in the presence and absence of the cells in the wells. The cell index was normalized to the baseline reading at time point 0, following attachment. Cellular impedance was measured periodically every 5 min. The electronic sensors provided a continuous and quantitative measurement of the cell index (which depends on the number of attached cells and the shape of the cells) in each well. Cell proliferation measured using the cell index was monitored for 72 h. For primary human TNBC breast cancer cells, 10 or 20 μM alisol A was used to confirm the effects of alisol A on breast cancer cells.

Colony-formation assay. Colony-formation assay was performed to determine the inhibitory effect of alisol A on MDA-MB-231 cells. Briefly, following treatment with 10 μM *Alisma orientale* compounds or 5, 10 or 20 μM alisol A treatment for 24 h, cells were detached using 0.25% trypsin, resuspended, plated at the density of $1x10^3$ cells per 10 cm dish (Corning Inc.), and incubated for 24 h. This was followed by the addition of alisol A. After 10 days, the cells were fixed with

4% methanol-free formalin (Sigma-Aldrich; Merck KGaA) for 10 min and permeabilized with pure methanol (Sigma-Aldrich; Merck KGaA) for 10 min at room temperature. Then, the cells were stained with 0.5% crystal violet (Sigma-Aldrich; Merck KGaA) for 10 min and washed with Dulbecco's phosphate buffered saline (DPBS; Welgene) slowly at room temperature until the crystal violet in the background was washed. The number of colonies was counted using ImageJ 1.8.0 (NIH).

Cell apoptosis assay. MDA-MB-231 cells ($1x10^5$ cells) were seeded in 6-well plates. After treatment with 5, 10 or 20 μM alisol A for 24 h, an Annexin V-FITC/propidium iodide (PI) double-staining Apoptosis Detection kit (Becton, Dickinson and Company) was used to label the cells, according to the manufacturer's instructions. MDA-MB-231 cells treated with dimethyl sulfoxide (DMSO, 0.1% (v/v)) were used as negative control. Cells were washed twice with cold PBS, and then resuspended in 200 μl Annexin V binding buffer at room temperature. After the cells were stained with 10 μl FITC-labeled Annexin V and 5 μl PI at room temperature for 15 min in the dark, the samples were immediately analyzed using flow cytometry (Becton Dickinson FACS Calibur; Becton, Dickinson and Company).

Terminal deoxynucleotidyl transferase-mediated dUTP nick-end labeling (TUNEL) assay. To determine the effects of alisol A on DNA fragmentation in MDA-MB-231 cells, a DeadEnd™ fluorometric terminal deoxynucleotidyl transferase (TdT)-mediated dUTP nick-end labeling (TUNEL) system (Promega Corporation) was used. The TUNEL assay was processed according to the manufacturer's instructions. Cell nuclei was stained with 4'6-diamidino-2-phenylindole (DAPI) at room temperature for 10 min.

Cell cycle analysis. The MDA-MB-231 cells ($1x10^5$ cells) were seeded in 6-well plates. After treatment with 5, 10 or 20 μM alisol A for 24 h, the cells were harvested and washed twice with cold PBS. MDA-MB-231 cells treated with DMSO of 0.1% (v/v) were used as negative control. The cells were suspended in 0.5 ml 70% (v/v) ethanol and chilled at -20˚C for 24 h. After extensive washing with PBS, the cells were resuspended in PBS containing 10 μg/ml 7-amino-actinomycin D (7AAD) (BD Biosciences) and 0.1 mg/ml RNase A and incubated at 37˚C for 30 min. The cells were subsequently resuspended in PBS and analyzed using flow cytometry (Becton Dickinson FACS Calibur). The results were analyzed using ModFit LT 3.2 Software (Verity Software House, Inc.).

Measurement of intracellular ROS. Intracellular ROS levels were measured using a cell-permeable fluorogenic probe as described previously (13). Briefly, after treatment with alisol A, cells were washed with PBS and the ROS levels were monitored using a 2',7'-dichlorodihydrofluorescein diacetate (DCF-DA) molecular probe (Beyotime Institute of Biotechnology). The DCF fluorescence distribution in the cells was observed under a fluorescence microscope (Olympus Corporation) at x200 magnification.

Immunofluorescence staining and confocal microscopy. Immunofluorescence was performed as previously described (14). After treatment with 5, 10 or 20 μM alisol A for 24 h, the cells were washed with PBS, and then fixed using 4% paraformaldehyde in PBS (pH 7.4) at room temperature for 30 min. This was followed by permeabilizing with 0.5% Triton X-100 on ice for 30 min, followed by blocking for 1 h in 1% bovine serum albumin solution at room temperature. The cells were then incubated overnight with primary antibodies against APE1 (cat. no. sc-17774; 1:100; Santa Cruz Biotechnology, Inc.), γH2AX (cat. no. 9718; 1:400; Cell Signaling Technology, Inc.), and LC3-II (cat. no. 2775; 1:200; Cell Signaling Technology, Inc.) at 4˚C. After washing three times with PBS containing 0.1% Tween-20 and 0.01% Triton X-100 for 5 min each, the cells were incubated with an appropriate FITC-conjugated secondary IgG including Alexa Fluor 594 anti-rabbit IgG (cat. no. A21207; 1:700; Invitrogen; Thermo Fisher Scientific, Inc.) and Alexa Fluor 488 anti-mouse IgG (cat. no. A11029; 1:700; Invitrogen; Thermo Fisher Scientific, Inc.) for 1 h at room temperature in the dark. After the nuclei were stained with DAPI at room temperature for 5 min, the cells were washed several times. Finally, observation was performed under a confocal laser scanning microscope (CLSM 710; Zeiss AG) at x400 magnification.

Western blotting. Proteins associated with cell cycle, apoptosis, and autophagy were detected by western blot analysis. Cells treated with alisol A or negative control cells were harvested individually. For protein extraction, cells were suspended in Cell lysis buffer for Western (cat. no. P0013; Beyotime Institute of Biotechnology) containing a protease inhibitor mixture and shaken on ice for 30 min. The cell lysate was centrifuged at 15,000 x g at 4˚C for 10 min, and the supernatant was collected. The total protein concentration was measured using the Bradford method or the bicinchoninic acid (BCA) protein assay kit. Proteins (40 μg) were separated on 12% (w/v) SDS-PAGE gels and electrophoretically transferred onto polyvinylidene difluoride membranes (EMD Millipore). The membranes were blocked in 5% (w/v) fat-free milk in Tris-buffered saline-0.5% (v/v) Tween-20 at room temperature for 1 h and incubated overnight at 4˚C with antibodies against caspase-3 (1:1,000; cat. no. 9662S; Cell Signaling Technology, Inc.), caspase-9 (1:1,000; cat. no. 9502S; Cell Signaling Technology, Inc.), Bcl-2 (1:1,000; cat. no. 15071S; Cell Signaling Technology, Inc.), p-p38 (1:100; cat. no. sc-166182; Santa Cruz Biotechnology, Inc.), cyclin A (1:100; cat. no. sc-271682; Santa Cruz Biotechnology, Inc.), cyclin D1 (1:500; cat. no. K0062-3; MBL International Co.), LC3-II (1:1,000; cat. no. 2775; Cell Signaling Technology, Inc.) or GAPDH (1:200; cat. no. sc-47724; Santa Cruz Biotechnology, Inc.). After three washes with PBS supplemented with 0.1% (v/v) Tween-20 (PBST) for 15 min, the membranes were incubated with goat anti-rabbit IRDye 680RD (1:5,000; cat. no. 926-68071; LI-COR Biosciences) or goat anti-mouse IRDye 800CW (1:5,000; cat. no. 926-32210; LI-COR Biosciences) for 1 h at room temperature. Proteins were identified by scanning the membranes using the Odyssey Imager (LI-COR Biosciences). ImageJ 1.8.0 (National Institutes of Health) was used to quantify the protein bands.

Statistical analysis. Data are presented as the mean ± standard deviation (SD) of three independent experiments. The

significance of differences were analyzed using one-way analysis of variance (ANOVA) and post-hoc Tukey's test. The half maximal inhibitory concentration (IC_{50}) of alisol A was calculated using Probit regression. All statistical analyses were performed using SPSS 23.0 software (IBM Corp.). $P<0.05$ was considered to indicate a statistically significant difference.

Results

Effects of Alismatis Rhizoma compounds on breast cancer cells viability. TNBC MDA-MB-231 cells were used to evaluate the cytotoxicity of Alismatis Rhizoma compounds on human breast cancer. Real-time cell proliferation assay and colony-formation assay were performed to evaluate the cytotoxicity of the four major protostane triterpenes of Alismatis Rhizoma. As shown in Fig. 1A and B, treatment with 10 μM alisol A, alisol A 24-acetate, alisol B, and alisol B 23-acetate for 24 h inhibited cell proliferation. Among them, alisol A was the most effective compound, which was investigated further in this study. The results of the real-time cell proliferation assay and colony-formation assay showed that the viability of MDA-MB-231 cells decreased dose-dependently after treatment with alisol A (Fig. 1C and D. Primary human TNBC cells were further used to confirm the effects of alisol A on breast cancer cells. As shown in Fig. S2, after treatment with 10 or 20 μM alisol A, the cell viability of primary human breast cancer cells decreased dose-dependently. Following treatment with 30 μM alisol A, cell proliferation at 80 h was inhibited to the baseline level, which is indicative of cell death. As a result, 20 μM was the highest concentration used in subsequent experiments. The IC_{50} of alisol A was 8.112 μM.

Alisol A induces apoptosis in breast cancer cells. To evaluate whether alisol A can induce cell apoptosis in MDA-MB-231 cells, annexin V/PI staining assay and TUNEL assay were used. After treatment with 5, 10 or 20 μM alisol A, the percentages of apoptosis-positive cells were 24.97±0.80, 31.81±0.36, or 33.87±0.65%, respectively, compared with 9.07±0.51% in the negative control group (Fig. 2A). The results (Fig. 2A and B) indicated that compared with the negative control, alisol A induced significant apoptosis in MDA-MB-231 cells 24 h post-treatment; the cell apoptotic effect was dose-dependent of alisol A. Alisol A (20 μM) was used to confirm the involvement of caspase activation in apoptosis, and activation of caspase-3 and caspase-9 was detected (Fig. 2C). Apoptosis-associated proteins, phosphorylated (p)- p38 was increased, and Bcl-2 was downregulated, which was consistent with the enhancement of apoptosis.

Alisol A induces G_1 phase cell cycle arrest in breast cancer cells. Cell cycle analysis showed that alisol A effectively induced G_1 phase cell cycle arrest in human breast cancer MDA-MB-231 cells. After 24 h exposure to 5 μM of alisol A, the fraction of cells in the G1 phase increased from 26.67±1.45 to 38.67±0.88%. When treated with 10 or 20 μM alisol A, the fraction of cells in the G_1 phase increased to 40.33±0.88 and 42.01±1.15%, respectively (Fig. 3A). This indicated that 5, 10 or 20 μM alisol A can induce G_1 phase cell cycle arrest. To further investigate alisol A-mediated G_1 phase arrest, the level of some associated proteins was detected using western blotting. Consistent with the results of the cell cycle analysis, the levels of cyclin A and cyclin D1 were decreased after treatment with alisol A for 24 h (Fig. 3B).

Alisol A induces autophagy in breast cancer cells. Recent reports have shown that autophagy can stimulate apoptosis (15). LC3-II expression was determined to evaluate the effect of alisol A on the induction of autophagy. LC3-II level increased significantly after treatment with alisol A. Further, the increase in LC3-II level was dose-dependent. In the negative control group, LC3-II was not detected. In the 20 μM alisol A treatment group, almost all cells showed LC3-II positivity (Fig. 4A). Western blot analysis showed that the level of LC3-II increased when treated with alisol. LC3-II expression was up-regulated three-fold when treated with 20 μM alisol A (Fig. 4B).

Alisol A induced ROS and DNA damage in breast cancer cells. DNA damage can promote cell autophagy and induce cell apoptosis via activation of the caspase pathway (16). Intracellular ROS level was assayed to obtain insights into the events underlying the mechanism of action of alisol A in breast cancer cells. Cells were treated with 5, 10, or 20 μM alisol A, and ROS levels were measured after treatment with the DCF-DA molecular probe. As shown in Fig. 5A, the ROS levels in the MDA-MB-231 cells were significantly higher in alisol A-treated cells than in the negative control cells ($P<0.01$), and the effect was dose-dependent. To investigate whether ROS induced oxidative DNA damage in alisol A-treated cells, apurinic/apyrimidinic endonuclease 1 (APE1), a surrogate marker of DNA single-strand breaks, and phosphorylated H2AX (γH2AX), a surrogate marker of DNA double-strand breaks, were assessed using immunofluorescence microscopy. As shown in Fig. 5B, the fractions of APE1- and γH2AX-positive cells increased significantly.

Discussion

More than 2 million cases of breast cancer were diagnosed in 2018, and more than 626,000 people succumbed to breast cancer, establishing breast cancer as the second most common cancer and the third most common cause of cancer-associated deaths worldwide (1). Furthermore, TNBC is characterized by the lack of targeted therapeutic receptors, due to which treatment options are limited. Therefore, the identification of new therapeutic agents for breast cancer is urgently required. Natural products can be potentially used for cancer therapies due to their significant effectiveness and low toxicity (17-19). Many anticancer drugs, such as paclitaxel and vincristine, are natural products of herbal origin, which play important roles in current chemotherapy (20).

Alisols, triterpenes belonging to the protostane family, are known as the major bioactive ingredients of Alismatis Rhizoma (21). Reports indicate that alisol derivatives possess many types of biological activities. However, the mechanisms via which these compounds act on breast cancer remains unclear. In the present study, the cytotoxicity of four major alisols of Alismatis Rhizoma, including alisol A, alisol A 24-acetate, alisol B, and alisol B 23-acetate was first screened. The data showed that alisol A had significant

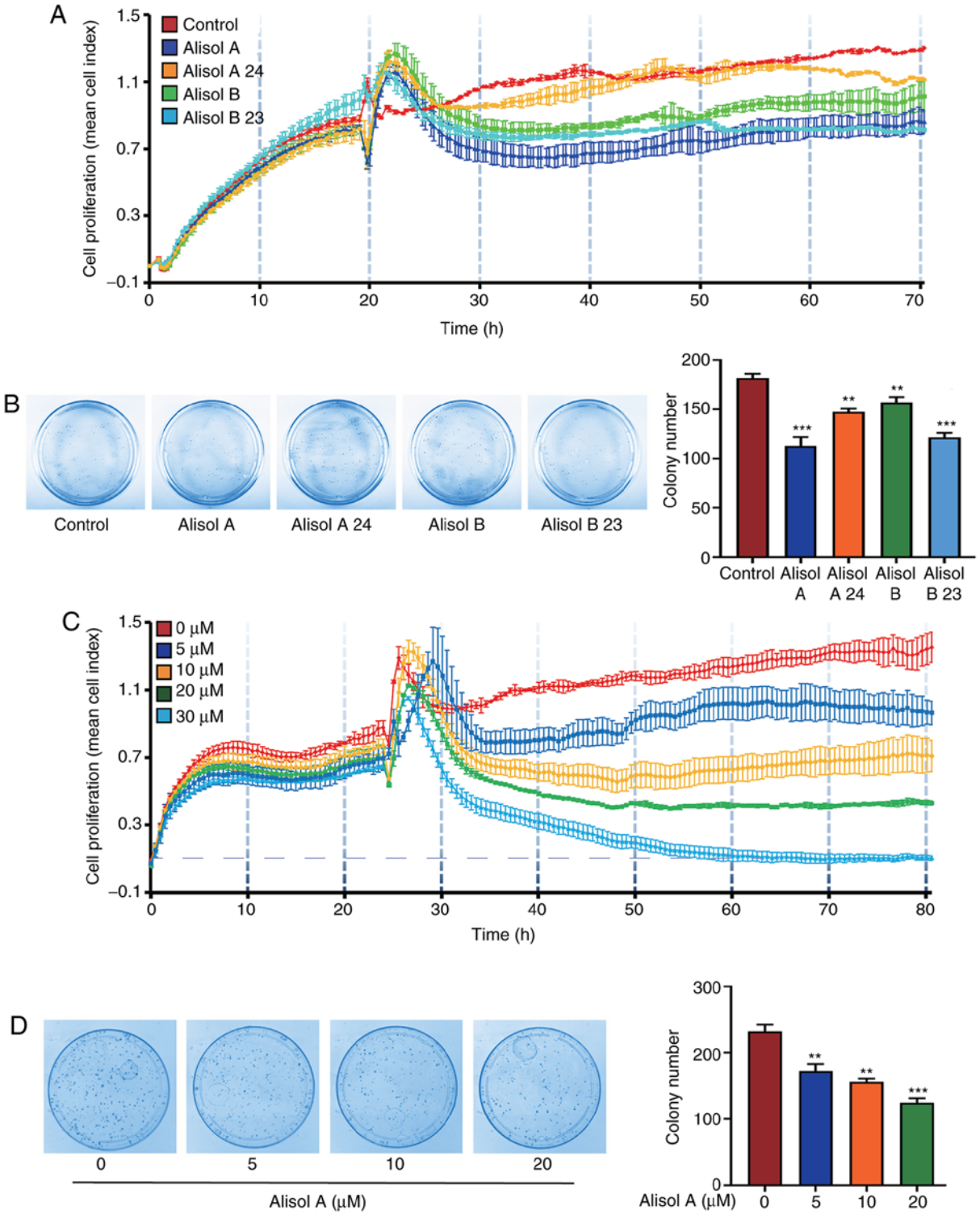

Figure 1. Alisol A decreases the cell viability of breast cancer MDA-MB-231 cells. (A and B) MDA-MB-231 cells were treated with 10 μM Alismatis Rhizoma compounds for 24 h, and the cell viability was assessed using a real-time cell proliferation assay and colony-formation assay, respectively. (C and D) MDA-MB-231 cells were treated with different concentrations of alisol A, and the cell viability was assessed using a real-time cell proliferation assay and colony-formation assay, respectively. Data are shown as mean ± SD of three independent experiments. **P<0.01; ***P<0.001 vs. control.

antitumor activity against breast cancer MDA-MB-231 cells, a TNBC cell line. To comprehensively explore the changes in alisol A-treated cells, cell apoptosis, cell cycle, and autophagy were measured. ROS levels and DNA damage were measured to identify whether these cellular changes were associated with oxidative DNA damage, which is a critical inducer of cell death, and can be utilized for selective cancer therapy (22).

In the present study, MDA-MB-231 cells were used to investigate the potential therapeutic effects of alisol A on TNBC. The results showed that alisol A can significantly inhibit the proliferation of MDA-MB-231 cells, using a real-time cell

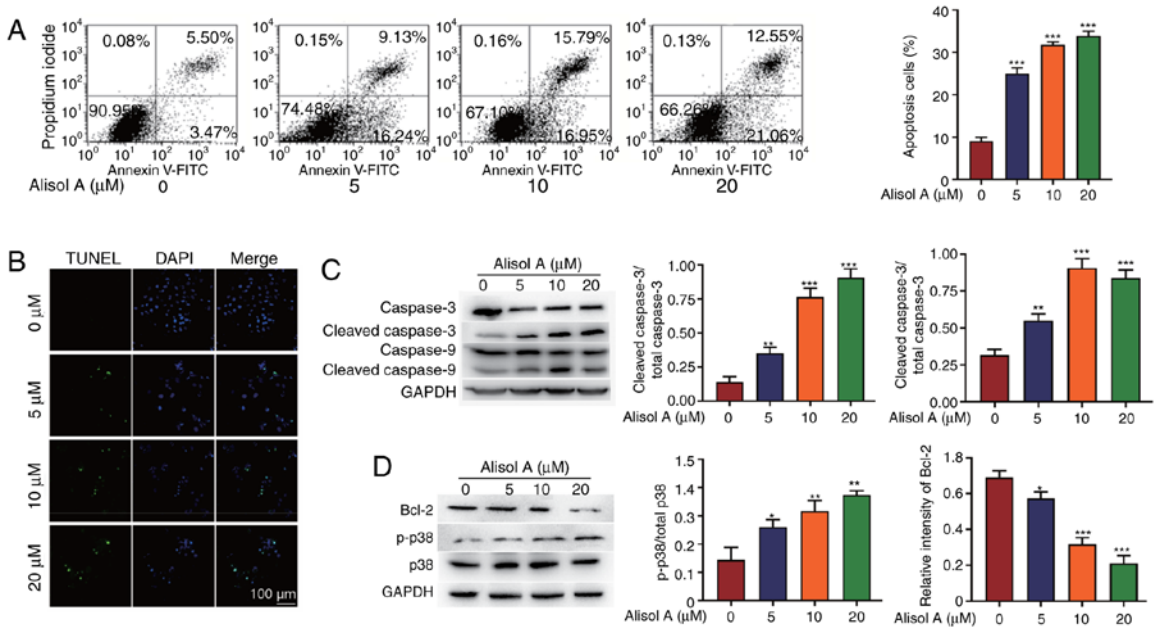

Figure 2. Alisol A induces cell apoptosis in breast cancer MDA-MB-231 cells. (A) Annexin V/PI staining assay was conducted using flow cytometry, and the extent of apoptosis was calculated. (B) TUNEL assay was conducted to determine DNA fragmentation in MDA-MB-231 cells. (C and D) Effects of alisol A on the proteins associated with apoptosis in MDA-MB-231 cells. Cells were incubated with alisol A for 24 h, and cell lysates were subjected to western blot analysis for caspase-3, caspase-9 (C); Bcl-2, and p-p38 (D). GAPDH was used as the control. Data are shown as mean ± SD of three independent experiments. **P<0.01; ***P<0.001 vs. control.

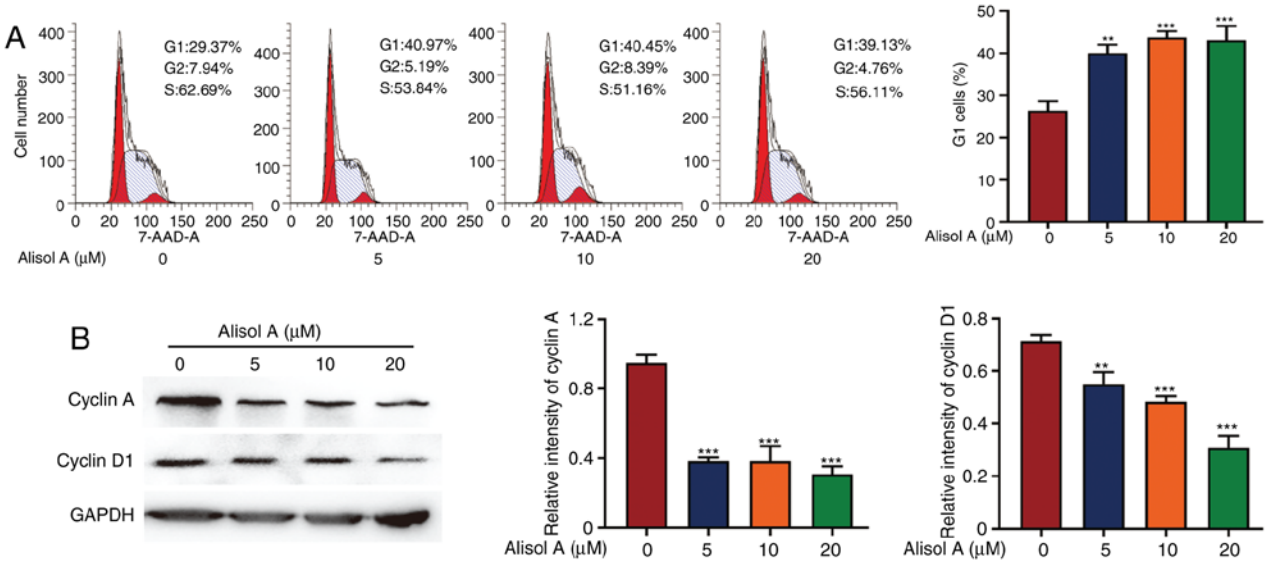

Figure 3. Alisol A induces G_1 phase cell cycle arrest in breast cancer MDA-MB-231 cells. (A) Cells at G_1 phase were tested and analyzed using flow cytometry assay. (B) Proteins levels of cyclin A and cyclin D1 were measured using western blot analysis. Cells were incubated with alisol A for 24 h and the cell lysates were subjected to western blot analysis for cyclin A and cyclin D1. GAPDH was used as the control. Data are shown as mean ± SD of three independent experiments. **P<0.01; ***P<0.001 vs. control.

proliferation assay that measured the cell index in real time. While analyzing the cellular changes induced by alisol A treatment, it was observed that the percentage of apoptotic cells increased. Resistance to apoptosis is a major obstacle leading to chemotherapy failure during cancer treatment (23). Drugs that can circumvent this obstacle will be effective for cancer therapy. Moreover, the results showed that cleaved caspase-3 and caspase-9 were activated, which can trigger cell apoptosis. A recent study reported that caspase-3 activation can offer insights into cancer chemotherapy (24). Bcl-2 protein was found to be downregulated after alisol A treatment. Bcl-2, as an anti-apoptotic protein, could control mitochondrial outer membrane permeabilization and has also been reported to be involved in chemotherapy-induced cell death (25). Alisol A treatment increased p-p38 level in MDA-MB-231 cells, which plays critical roles in mediating cellular response to stressors, and is involved in the p38-MAPK signaling pathway, thereby linking apoptosis with ROS production (26). Previous studies

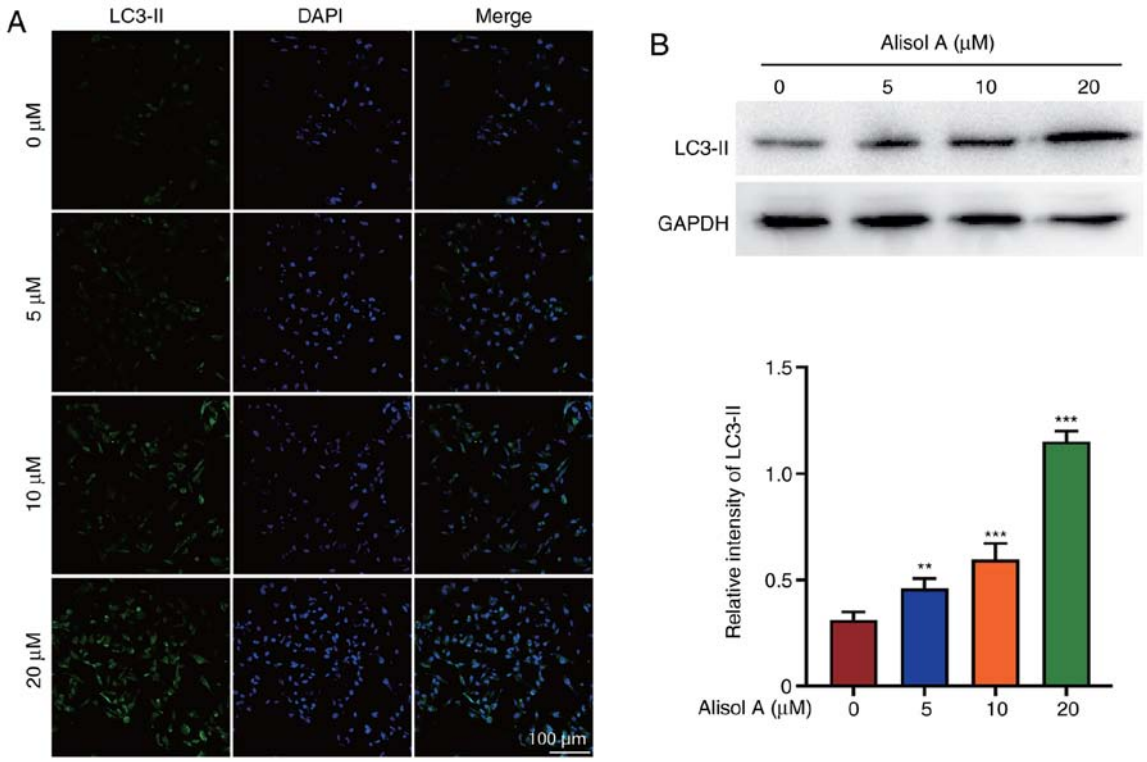

Figure 4. Alisol A induces autophagy in human breast cancer MDA-MB-231 cells. (A) MDA-MB-231 cells were treated with alisol A for 24 h. Representative images showing LC3-II fluorescence. (B) LC3-II protein levels were measured using western blot analysis. GAPDH was used as the control. Data are show as mean ± SD of three independent experiments. **P<0.01; ***P<0.001 vs. control.

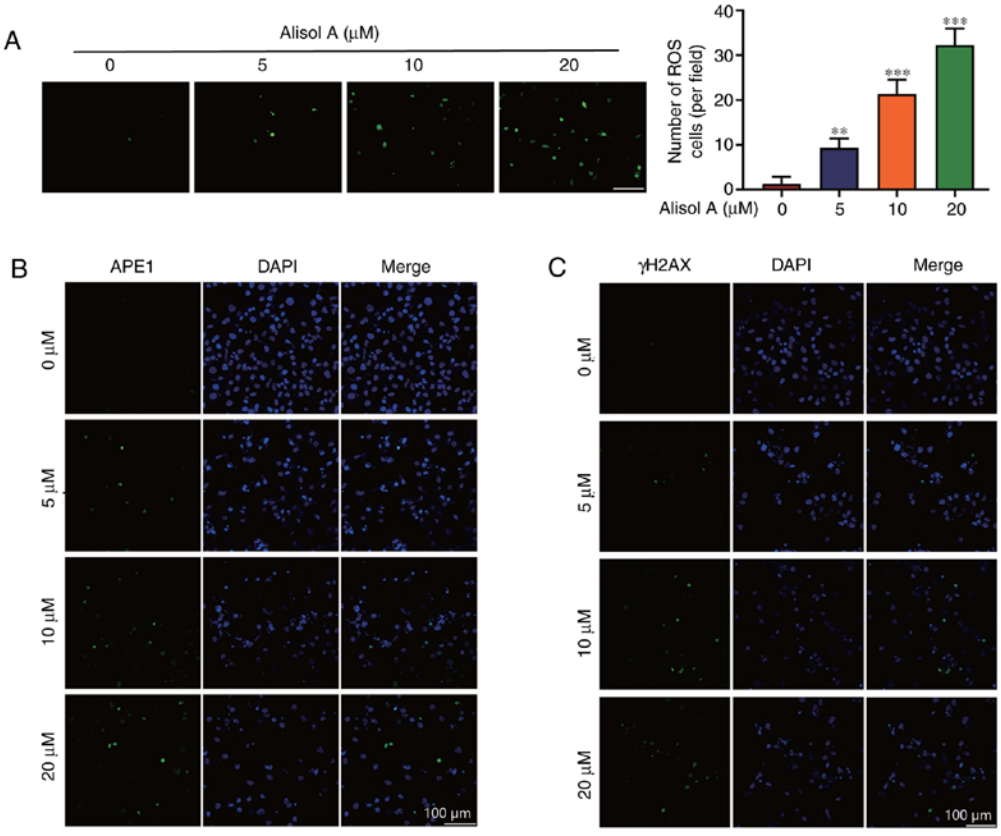

Figure 5. Alisol A induces intracellular ROS and DNA damage in human breast cancer MDA-MB-231 cells. (A) After cells were treated with alisol A for 24 h, the intracellular ROS levels in the breast cancer MDA-MB-231 cells were measured after DCF-DA molecular probe treatment, followed by fluorescence microscopy. Statistical analysis of ROS-positive cells per field are shown. (B) APE1 and (C) γH2AX expression was measured using immunofluorescence microscopy, after cells were treated with alisol A. Data are shown as the mean ± SD of three independent experiments. **P<0.01; ***P<0.001 vs. control. ROS, reactive oxygen species; APE1, apurinic/apyrimidinic endonuclease 1.

have shown that p38 is involved in the p38-MAPK signaling pathway and its activation is associated with cell apoptosis in different tissues (27-31). In the present study, the expression of the members of this signaling pathway was assessed. It was found that following alisol A treatment, intracellular ROS and DNA damage were induced, p38 was activated, and Bcl-2 was inhibited, which activated the mitochondrial apoptotic caspase cascade, including caspase-9/3.

Cell cycle arrest at the G_1 phase is one of the main triggers of apoptosis. It was found that the number of cells at the G_1 phase was increased after alisol A treatment, indicating that the G_1 cell cycle arrest was induced by alisol A. Cyclin A and cyclin D1, the two critical molecules involved in controlling cell cycle progression, were downregulated by alisol A treatment. Cyclins function as regulators of CDK to regulate mitotic events. Cyclin D1 acts to control the G_1/S transition by regulating the activity of CDK4/CDK6. Defects in cyclin D1, which is under the complex regulation of upstream proteins, is sufficient to induce abnormal G_1/S transition and G_1 cell cycle arrest (32,33). In addition, cyclin A interacts with CDK2 to control DNA synthesis, and hence, defects in cyclin A lead to the G_1/S arrest (34,35). Cell cycle arrest and induction of apoptosis are the two major causes for suppression of cell proliferation (19).

Basal levels of autophagy could ensure the physiological turnover of damaged organelles, while a large accumulation of autophagic vacuoles may induce cell death. Autophagy, which is induced in response to many types of stress, including chemotherapeutic intervention, could ultimately lead to apoptosis (36). Several types of interactions between apoptosis and autophagy have been described, indicating a complex mechanistic overlap and interaction between the apoptotic mechanisms and autophagy-associated proteins (37). Apoptosis may begin with autophagy, and autophagy often culminates in apoptosis. When autophagy is induced, LC3-I is converted to LC3-II, which is an important autophagosome marker (38). It found that alisol A promoted the induction of autophagy in breast cancer cells.

The induction of DNA damage is considered to be one of the important mechanisms of action of cancer therapeutics (39). Previously, ROS has been reported to induce oxidative DNA damage (13). Whether alisol A enhanced the efficacy of cancer therapy via induction of ROS and oxidative DNA damage remains unclear. In the present study, it was shown that alisol A increased intracellular ROS levels and induced APE1 and γH2AX accumulation in breast cancer cells. As previously described, APE1 is a critical regulator of the cellular response to ROS and is well known for the DNA backbone cleavage activity during base excision repair, while γH2AX is required for the stabilization of various DNA damage response factors at the sites of DNA lesions (13). DNA-damaging drugs are commonly used in cancer therapy. Studies on the role of DNA damage response in drug discovery are essential for identifying novel cancer therapeutic options (39). The findings of the present study indicate that alisol A could play an efficient role against breast cancer via the induction of ROS and DNA damage. Thus, alisol A could offer a new therapeutic option for breast cancer.

In conclusion, the present study suggests that alisol A from Alismatis Rhizoma may be used as a novel agent for breast cancer therapy. The results are consistent with the observations of a previous study on the effects of alisol A on breast cancer cells (40). More cell lines should be used to confirm the effects of alisol A, to validate its potential of therapeutic effect. As reported previously, different cell lines were used to show the effects of alisol A (40). The results showed that MDA-MB-231 cell line was the most significant cell line (40). The present study was a pilot study that screened the cytotoxicity of four major alisols of Alismatis Rhizoma, including alisol A, alisol A 24-acetate, alisol B and alisol B 23-acetate. According to the previous study (40), MDA-MB-231 cell line was first used to attain the primary goal. After screening, primary human TNBC cells were used to confirm the effects of alisol A on breast cancer cells, as shown in Fig. S2. The present study demonstrated that the alternative induction of ROS and DNA damage was the mechanism underlying alisol A-induced cellular changes, which has not been previously reported. Further studies using animal models are required to confirm the functions of alisol A in breast cancer therapy.

Acknowledgements

Not applicable.

Funding

This study was funded by the National Natural Science Foundation of China (grant nos. 81672610 and 81872978), and Major National Science and Technology Project of China (gra nt no. 2014ZX09304307-001-011).

Availability of data and materials

The datasets used and/or analyzed during the current study are available from the corresponding author on reasonable request.

Authors' contributions

YS, MW and PW performed the experiments and wrote the manuscript. TZ performed the western blot analysis. JY and LS performed the experiments for protostane triterpenes purification and assessment. ML, HW, QZ and HZ designed the study. All authors read and approved the final version of the manuscript.

Ethics approval and consent to participate

The use of human specimens in the present study was approved by the Peking University Third Hospital Medical Science Research Ethic Committee (approval no. IRB00006761-M20 19343). Informed consent was obtained from all the patients.

Patient consent for publication

Not applicable.

Competing interests

The authors declare that they have no competing interests.

References

1. Bray F, Ferlay J, Soerjomataram I, Siegel RL, Torre LA and Jemal A: Global cancer statistics 2018: GLOBOCAN estimates of incidence and mortality worldwide for 36 cancers in 185 countries. CA Cancer J Clin 68: 394-424, 2018.
2. DeSantis C, Ma J, Bryan L and Jemal A: Breast cancer statistics, 2013. CA Cancer J Clin 64: 52-62, 2014.
3. Torre LA, Islami F, Siegel RL, Ward EM and Jemal A: Global cancer in women: Burden and trends. Cancer Epidemiol Biomarkers Prev 26: 444-457, 2017.
4. Chae SY, Ahn SH, Kim SB, Han S, Lee SH, Oh SJ, Lee SJ, Kim HJ, Ko BS, Lee JW, *et al*: Diagnostic accuracy and safety of 16alpha-[(18)F]fluoro-17β-oestradiol PET-CT for the assessment of oestrogen receptor status in recurrent or metastatic lesions in patients with breast cancer: A prospective cohort study. Lancet Oncol 20: 546-555, 2019.
5. Venkitaraman R: Triple-negative/basal-like breast cancer: Clinical, pathologic and molecular features. Expert Rev Anticancer Ther 10: 199-207, 2010.
6. Shi J, Kantoff PW, Wooster R and Farokhzad OC: Cancer nanomedicine: Progress, challenges and opportunities. Nat Rev Cancer 17: 20-37, 2017.
7. Jiang YZ, Ma D, Suo C, Shi J, Xue M, Hu X, Xiao Y, Yu KD, Liu YR, Yu Y, *et al*: Genomic and transcriptomic landscape of triple-negative breast cancers: Subtypes and treatment strategies. Cancer Cell 35: 428-440.e5, 2019.
8. Li M, Huang T, Li MJ, Zhang CX, Yu XC, Yin YY, Liu C, Wang X, Feng HW, Zhang T, *et al*: The histone modification reader ZCWPW1 is required for meiosis prophase I in male but not in female mice. Sci Adv 5: eaax1101, 2019.
9. Newman DJ and Cragg GM: Natural products as sources of new drugs over the 30 years from 1981 to 2010. J Nat Prod 75: 311-335, 2012.
10. Liao M, Shang H, Li Y, Li T, Wang M, Zheng Y, Hou W and Liu C: An integrated approach to uncover quality marker underlying the effects of Alisma orientale on lipid metabolism, using chemical analysis and network pharmacology. Phytomedicine 45: 93-104, 2018.
11. Zhang L, Xu W, Xu YL, Chen X, Huang M and Lu J: Therapeutic potential of rhizoma alismatis: A review on ethnomedicinal application, phytochemistry, pharmacology, and toxicology. Ann N Y Acad Sci 1401: 90-101, 2017.
12. Tian T, Chen H and Zhao YY: Traditional uses, phytochemistry, pharmacology, toxicology and quality control of Alisma orientale (Sam.) Juzep: A review. J Ethnopharmacol 158: 373-387, 2014.
13. Shi Y, Wang P, Guo Y, Liang X, Li Y and Ding S: Helicobacter pylori-induced DNA damage is a potential driver for human gastric cancer AGS cells. DNA Cell Biol 38: 272-280, 2019.
14. Liang X, Jin Y, Wang H, Meng X, Tan Z, Huang T and Fan S: Transgelin 2 is required for embryo implantation by promoting actin polymerization. FASEB J 33: 5667-5675, 2019.
15. Kasprowska-Liśkiewicz D: The cell on the edge of life and death: Crosstalk between autophagy and apoptosis. Postepy Hig Med Dosw (Online) 71: 825-841, 2017.
16. Li B, Chen R, Chen L, Qiu P, Ai X, Huang E, Huang W, Chen C, Liu C, Lin Z, *et al*: Effects of DDIT4 in methamphetamine-induced autophagy and apoptosis in dopaminergic neurons. Mol Neurobiol 54: 1642-1660, 2017.
17. Luo F, Gu J, Chen L and Xu X: Systems pharmacology strategies for anticancer drug discovery based on natural products. Mol biosyst 10: 1912-1917, 2014.
18. Crrowell JA: The chemopreventive agent development research program in the division of cancer prevention of the US National Cancer Institute: An overview. Eur J Cancer 41: 1889-1910, 2005.
19. Chen X, Wu QS, Meng FC, Tang ZH, Chen X, Lin LG, Chen P, Qiang WA, Wang YT, Zhang QW and Lu JJ: Chikusetsusaponin IVa methyl ester induces G1 cell cycle arrest, triggers apoptosis and inhibits migration and invasion in ovarian cancer cells. Phytomedicine 23: 1555-1565, 2016.
20. de Fátima A, Terra BS, da Silva CM, da Silva DL, Araujo DP, da Silva Neto L and Nascimento de Aquino RA: From nature to market: Examples of natural products that became drugs. Recent Pat Biotechnol 8: 76-88, 2014.
21. Murata T, Imai Y, Hirata T and Miyamoto M: Biological-active trieterpenes of Alismatis rhizoma. I. Isolation of the alisols. Chem Pharm Bull (Tokyo) 18: 1347-1353, 1970.
22. Nogueira V and Hay N: Molecular pathways: Reactive oxygen species homeostasis in cancer cells and implications for cancer therapy. Clin Cancer Res 19: 4309-4314, 2013.
23. Gong Y, Fan Z, Luo G, Yang C, Huang Q, Fan K, Cheng H, Jin K, Ni Q, Yu X and Liu C: The role of necroptosis in cancer biology and therapy. Mol Cancer 18: 100, 2019.
24. Wang Y, Gao W, Shi X, Ding J, Liu W, He H, Wang K and Shao F: Chemotherapy drugs induce pyroptosis through caspase-3 cleavage of a gasdermin. Nature 547: 99-103, 2017.
25. Gonzalez PS, O'Prey J, Cardaci S, Barthet VJA, Sakamaki JI, Beaumatin F, Roseweir A, Gay DM, Mackay G, Malviya G, *et al*: Mannose impairs tumour growth and enhances chemotherapy. Nature 563: 719-723, 2018.
26. Huang J, Peng W, Zheng Y, Hao H, Li S, Yao Y, Ding Y, Zhang J, Lyu J and Zeng Q: Upregulation of UCP2 expression protects against LPS-induced oxidative stress and apoptosis in cardiomyocytes. Oxid Med Cell Longev 2019: 2758262, 2019.
27. Qian Z, Chang J, Jiang F, Ge D, Yang L, Li Y, Chen H and Cao X: Excess administration of miR-340-5p ameliorates spinal cord injury-induced neuroinflammation and apoptosis by modulating the P38-MAPK signaling pathway. Brain Behav Immun, 2020 (Epub ahead of print).
28. He J, Huang Z, He M, Liao J, Zhang Q, Wang S, Xie L, Ouyang L, Koeffler HP, Yin D and Liu A: Circular RNA MAPK4 (circ-MAPK4) inhibits cell apoptosis via MAPK signaling pathway by sponging miR-125a-3p in gliomas. Mol Cancer 19: 17, 2020.
29. Akter M, Jangra A, Choi SA, Choi EH and Han I: Non-thermal atmospheric pressure bio-compatible plasma stimulates apoptosis via p38/MAPK mechanism in U87 malignant glioblastoma. Cancers (Basel) 12: 245, 2020.
30. Xu Y, Yao H, Wang Q, Xu W, Liu K, Zhang J, Zhao H and Hou G: Aquaporin-3 attenuates oxidative stress-induced nucleus pulposus cell apoptosis through regulating the P38 MAPK pathway. Cell Physiol Biochem 50: 1687-1697, 2018.
31. Wagner EF and Nebreda AR: Signal integration by JNK and p38 MAPK pathways in cancer development. Nat Rev Cancer 9: 537-549, 2009.
32. Santra MK, Wajapeyee N and Green MR: F-box protein FBXO31 mediates cyclin D1 degradation to induce G1 arrest after DNA damage. Nature 459: 722-725, 2009.
33. Masamha CP and Benbrook DM: Cyclin D1 degradation is sufficient to induce G1 cell cycle arrest despite constitutive expression of cyclin E2 in ovarian cancer cells. Cancer Res 69: 6565-6572, 2009.
34. Chen ZH, Jing YJ, Yu JB, Jin ZS, Li Z, He TT and Su XZ: ESRP1 induces cervical cancer cell G1-phase arrest via regulating cyclin A2 mRNA stability. Int J Mol Sci 20: 3705, 2019.
35. Zhang X, Liu J, Zhang P, Dai L, Wu Z, Wang L, Cao M and Jiang J: Silibinin induces G1 arrest, apoptosis and JNK/SAPK upregulation in SW1990 human pancreatic cancer cells. Oncol Lett 15: 9868-9876, 2018.
36. Booth LA, Tavallai S, Hamed HA, Cruickshanks N and Dent P: The role of cell signalling in the crosstalk between autophagy and apoptosis. Cell Signal 26: 549-555, 2014.
37. Delgado ME, Dyck L, Laussmann MA and Rehm M: Modulation of apoptosis sensitivity through the interplay with autophagic and proteasomal degradation pathways. Cell Death Dis 5: e1011, 2014.
38. Liu D, Wu H, Wang C, Li Y, Tian H, Siraj S, Sehgal SA, Wang X, Wang J, Shang Y, *et al*: STING directly activates autophagy to tune the innate immune response. Cell Death Differ 26: 1735-1749, 2019.
39. Almeida LC, Bauermeister A, Rezende-Teixeira P, Santos EAD, Moraes LAB, Machado-Neto JA and Costa-Lotufo LV: Pradimicin-IRD exhibits antineoplastic effects by inducing DNA damage in colon cancer cells. Biochem Pharmacol 168: 38-47, 2019.
40. Lou C, Xu X, Chen Y and Zhao H: Alisol A suppresses proliferation, migration, and invasion in human breast cancer MDA-MB-231 cells. Molecules 24: 3651, 2019.